High precision ground-based CCD photometry from the Next Generation Transit Survey

Daniel Bayliss[a], Sean M. O'Brien[b], Edward Bryant[c], Peter Wheatley[a], Richard West[a], James McCormac[a], Paul Chote[a], Sam Gill[a], David R. Anderson[a], Adam Wise[d], Ines Juvan-Beaulieu[d], Colin Coates[d], Edward Gillen[e,f], Alexis M. S. Smith[g], James S. Jenkins[h,i], Maximiliano Moyano[j], Douglas R. Alves[k], Matthew R. Burleigh[l], Michael R. Goad[l], Sarah L. Casewell[l], Jack Acton[l], Rosanna L. Tilbrook[l], Beth A. Henderson[l], and Alicia Kendall[l]

[a]Department of Physics, University of Warwick, Gibbet Hill Road, Coventry, CV4 7AL, UK
[b]Astrophysics Research Centre, School of Mathematics and Physics, Queen's University Belfast, Belfast, BT7 1NN, UK
[c]Mullard Space Science Laboratory, University College London, Holmbury St Mary, Dorking, Surrey, RH5 6NT, UK
[d]Andor Technology Ltd, Springvale Business Park, 7 Millennium Way, Belfast BT12 7AL
[e]Astronomy Unit, Queen Mary University of London, Mile End Road, London E1 4NS, UK
[f]Astrophysics Group, Cavendish Laboratory, J.J. Thomson Avenue, Cambridge CB3 0HE, UK
[g]Institute of Planetary Research, German Aerospace Center (DLR), Rutherfordstr. 2, 12489 Berlin, Germany
[h]Núcleo de Astronomía, Facultad de Ingeniería y Ciencias, Universidad Diego Portales, Av. Ejército 441, Santiago, Chile
[i]Centro de Astrofísica y Tecnologías Afines (CATA), Casilla 36-D, Santiago, Chile
[j]Instituto de Astronomía, Universidad Católica del Norte, Angamos 0610, 1270709, Antofagasta, Chile
[k]Departamento de Astronomia, Universidad de Chile, Casilla 36-D, Santiago, Chile
[l]School of Physics and Astronomy, University of Leicester, Leicester LE1 7RH, UK

ABSTRACT

The Next Generation Transit Survey (NGTS) has now been operating for six years, discovering and characterizing transiting exoplanets around bright stars. We outline the NGTS project, including the Andor CCD cameras used to perform high-precision time-series photometry. We quantify the photometric precision for a sample of over 20,000 bright star observations. We find for single NGTS telescope observations we achieve a 30-minute photometric precision of 400 ppm at low airmass. This is in good agreement with the photometric noise predicted using a four-component noise model. We find that the photometric noise for bright stars ($G < 12$) is dominated by atmospheric scintillation. We also present details of the NGTS multi-telescope observing mode, whereby 12 telescopes can be used simultaneously on a single target star to achieve a 30-minute photometric precision of 100 ppm. Finally, we describe a new generation scientific CMOS camera that we will be testing on-sky at the NGTS facility to determine if it can compete with state-of-the-art CCD cameras used for high precision bright star photometry.

Keywords: CCD, CMOS, Photometry, Visible, Exoplanets

Further author information: (Send correspondence to D.B.)
E-mail: d.bayliss@warwick.ac.uk, Telephone: 44 24761 50342

X-Ray, Optical, and Infrared Detectors for Astronomy X, edited by Andrew D. Holland, James Beletic
Proc. of SPIE Vol. 12191, 121911A · © 2022 SPIE · 0277-786X · doi: 10.1117/12.2628966

1. INTRODUCTION

1.1 Transiting Exoplanets

The concept of discovering exoplanets via photometric transits dates back at least 70 years.[1] The discovery of 51 Pegasi in 1995[2] showed some exoplanets had much shorter orbital periods than the Solar System planets, greatly increasing the prospects of detecting an exoplanet transit. Just four years later, the first transiting exoplanet was discovered orbiting the star HD209458.[3,4] In the following years teams began to discover transiting exoplanets by photometrically monitoring large regions of the sky; most successfully with the WASP[5] and HATNet/HATSouth[6,7] projects, which together have discovered over 300 transiting exoplanets. The value of these discoveries to our understanding of exoplanets has been enormous, as in addition to well measured masses and radii, these planet are amenable to study by techniques such as atmospheric transmission spectroscopy[8] and thermal emission phase curves.[9] The bulk of early JWST exoplanet targets come from the discoveries made from these surveys.[10]

Most of the exoplanets found from these ground-based transit surveys were gas giants with radii similar or greater than Jupiter, which present transit signals of the order of 1%. Discovering smaller planets was difficult in large part due to systematic noise in the photometry masking shallow transit signals.[11] The Kepler mission[12] showed that small radius, short period planets were relatively common around solar-type stars.[13] The goal of the Next Generation Transit Survey (NGTS[14]) is to deliver high precision photometry from the ground capable of detecting Neptune-radius transiting exoplanets that present transit signals on the order of 0.1%.

1.2 NGTS

NGTS is a robotic and fully automated 12 telescope facility situated at ESO's Paranal Observatory in Chile. The telescopes are housed in a custom built enclosure with a roll-off roof (see Figure 1). Each telescope consists of an ASA f/2.8 20 cm aperture Netwonian telescope on a fully-independent Optical Mechanics Inc equatorial fork mount. Each telescope is coupled to a 2 K×2 K Andor iKon-L 936 CCD camera. An image of an NGTS telescope showing the telescope tube, mount, and camera is featured in Figure 2. We set out more details relating to the camera in Section 2.1. NGTS operates using a custom filter covering 520 to 890 nm. The majority of imaging is carried out with an exposure time of 10 s. Full details of the NGTS facility and project are set out in the project paper[14] and on the NGTS webpage https://ngtransits.org.

The NGTS project began in 2016. In 2018 NGTS made its first exoplanet discovery with NGTS-1 b,[15] a Jupiter-sized exoplanet transiting a low mass star. Since then NGTS has gone on to discover more than 20 transiting exoplanets. Of particular note is NGTS-4 b,[16] a rare sub-Neptune-sized exoplanet lying within the so-called "Neptunian Desert".[17,18] NGTS-4 b is the shallowest transiting exoplanet ever discovered from a ground-based transit search.

Over the past 6 years NGTS has continued to discover transiting exoplanets by surveying the sky. NGTS has also been extended to operate in a targeted mode, monitoring transiting exoplanets or exoplanet candidates from the TESS mission.[19] In this paper we provide an overview of the NGTS photometry, and present a study of the photometric precision for bright stars. We also look to the future of the project, including multi-telescope observations and testing a scientific CMOS camera, as we continue to discover and characterise transiting exoplanets.

In Section 2 we outline our CCD cameras, autoguiding and aperture photometry that are at the core of producing high precision photometric data for the NGTS project. In Section 3 we present a study of the photometric noise in the NGTS data, comparing a four-component noise model to a large sample of bright star observations. In Section 4 we outline a new multi-telescope observing mode used at NGTS to achieve even higher precision photometry for targeted monitoring. In Section 5 we discuss an extension of the NGTS project to test a new state-of-the-art sCMOS camera for high precision photometry of bright stars. Finally in Section 6 we provide our conclusions.

Figure 1. The NGTS enclosure during dusk moon-rise at ESO's Paranal Observatory in Chile. The roll-off roof is open, allowing each of the 12 telescopes an unobstructed view of the night sky to an airmass of 2.0 (60° from zenith). Image credit: D. Bayliss

2. CCD PHOTOMETRY

2.1 iKon-L CCD Camera

To achieve high precision time-series photometry, NGTS relies on the images delivered by the iKon-L 936 CCD camera, as shown in Figure 2, manufactured by Andor Technology*. A number of design features make this camera ideal for high precision photometry, which we highlight in this section.

The iKon-L CCD has a sensor size of 27.6×27.6 mm and utilizes the back-illuminated BR-DD sensor option. Table 1 summarizes the main characteristics of the iKon-L CCD. The BR-DD camera model provides high quantum efficiency with fringe suppression and an ideal wavelength coverage for observations in the visible and near infrared. Figure 3 illustrates the quantum efficiency of this sensor alongside the NGTS filter bandpass of 520 to 890 nm. We also compare the sensitivity of the Andor Marana 4.2B-11 BV sCMOS camera, which is discussed in Section 5.

The BR-DD detector is a CCD42-40 non-inverted mode operation (NIMO) back-illuminated and deep-depletion sensor from Teledyne e2v†. Due to its NIMO characteristics, the dark current is higher than the one of a standard device. However, for the observations at NGTS this is negligible as the dark current remains much lower than the sky background.[14]

The 12 iKon-L CCDs at NGTS use 4-stage thermoelectric cooling, which allows for observations at an absolute sensor temperature of -70°C. This represents a favorable cooling temperature for observations with back-illuminated deep-depletion sensors in the 750-1000 nm region, as the quantum efficiency of some sensors, such as the BR-DD model, show a temperature dependence in near-infrared sensitivity. This results in a trade-off: as the sensor cools further, dark current decreases but so does long-wavelength quantum efficiency. A

*https://andor.oxinst.com/
†https://www.teledyne-e2v.com/

Table 1. Summary of technical specifications of the Andor iKon-L CCD and the Andor Marana BV-11 sCMOS

Description	**iKon-L 936 (CCD)**	**Marana BV-11 (sCMOS)**
Active pixels	2048 × 2048	2048 × 2048
Detector size	27.6×27.6 mm	22.5×22.5 mm
Pixel size	13.5×13.5 µm	11×11 µm
Read Noise	12 e- in fast readout mode (1.5 s)	1.6 e- in all readout modes
Dark Current	0.006 e-/pix/s at -80°C	0.7 e-/pixel/s at -25°C
Sensor Type	e2v BR-DD	GSense 400BSI
QE	peak QE > 95% at 800nm	peak QE > 95% at 550nm
Full Frame Readout Time	1.5 s	0.042 s
Operating temperature	-70°C	-25°C
Shutter	45 mm programable shutter	shutterless

consideration of signal to noise ratio versus measurement wavelength is required when deciding on a sensor cooling strategy.

The readout speed we use to operate the CCD is 3 MHz, which results in a readout time of 1.5 s for a full frame, and a read noise of around 12 electrons root-mean-square (RMS). The iKon-L also offers slower readout modes with lower read noise, however, this would lead to longer readout times and reduced on-sky exposure time.[14] Given that NGTS prioritises bright star photometry, it is more important to minimise the readout time. Figure 4 highlights that even with a read noise value of 12 electrons, this is only a very minor component for the

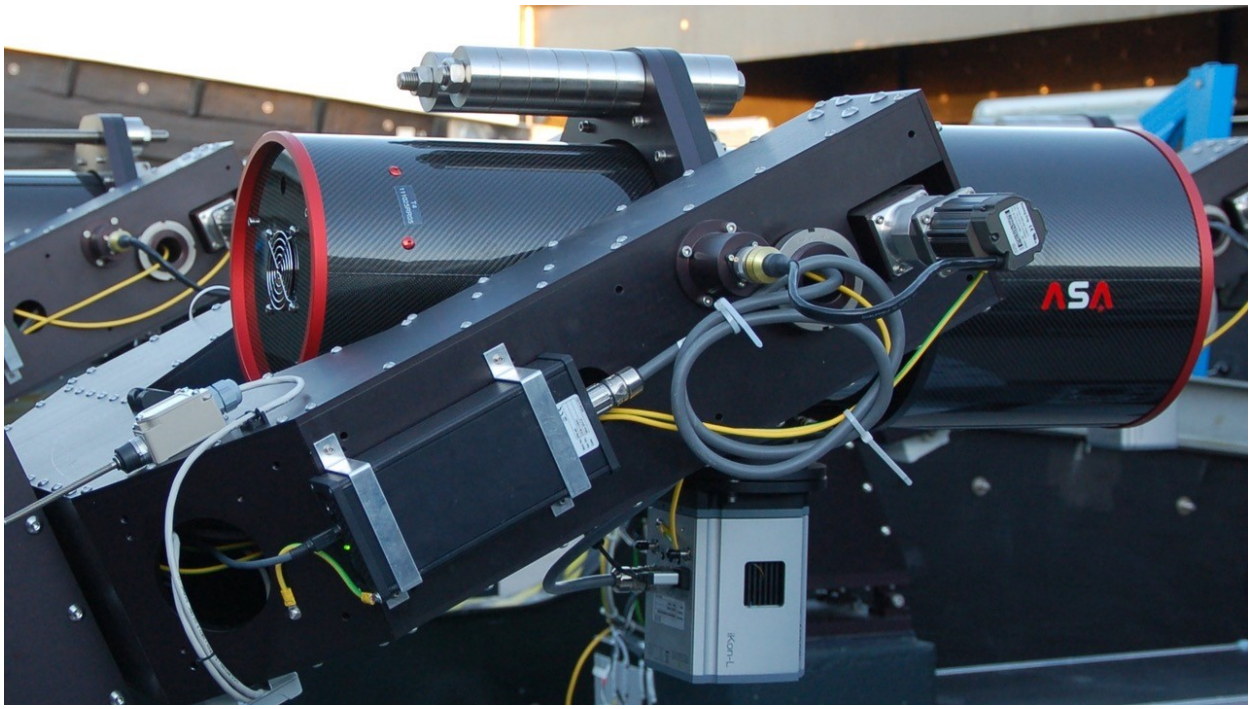

Figure 2. One of the 12 NGTS telescopes in the stowed position. Visible is the Optical Mechanics Inc equatorial fork mount holding the telescope, the carbon fibre ASA telescope tube, and the Andor iKon-L CCD camera mounted below the telescope tube. Image credit: D.Bayliss

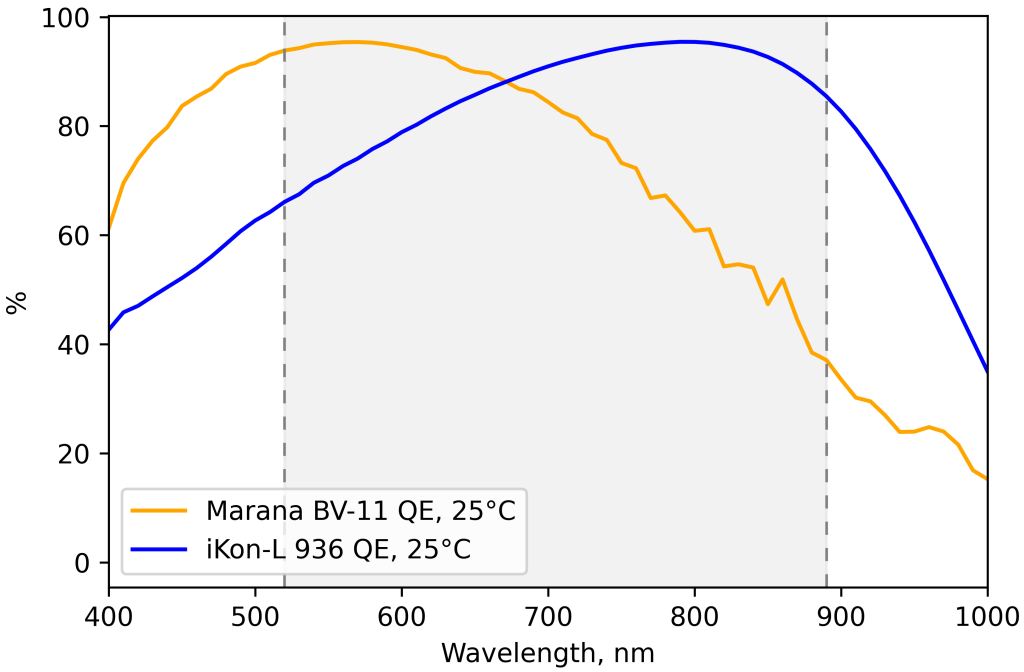

Figure 3. The quantum efficiency of the NGTS Andor iKon-L BR-DD CCD camera (blue solid curve) in relation to the NGTS filter bandpass (grey shaded region). Also plotted is the quantum efficiency curve for the Marana 4.2B-11 BV sCMOS discussed in Section 5.

photometric noise, even for fainter stars.

To better suit the specific aims of this project, NGTS and Andor Technology collaborated to create a modified version of the standard iKon-L CCD optimized for photometric precision. The customised NGTS cameras have a modified internal fan for improved thermal stability, re-designed readout electronics for reduced thermal sensitivity, and adjustable collection phase CCD voltage to maximise charge conservation at saturation.[14]

2.2 Autoguiding

In order to achieve high photometric precision, we maintain stars at precisely fixed positions on the CCD. We achieve this using a closed-loop autoguiding system that continuously makes small adjustments to the telescope pointing based on a real-time analysis of the science images. The system makes use of the DONUTS code[20] and maintains guiding to an RMS precision of around 0.03 pixels that is repeatable across timescales of months.[14]

2.3 Photometry

We produce high precision photometry from the individual CCD image frames using simple aperture photometry whereby all pixels within a fixed radius of the target star are summed. For the original NGTS transit survey this was performed by a custom photometric pipeline.[14] For the targeted bright star observations, we use a stand-alone photometric pipeline[21] based on the SEP.[22] Interestingly we found that traditional image calibration using bias, dark, and flat-field frames does *not* improve our bright star photometric precision. The bias frames show little variation or structure and the dark current is extremely low (see Section 2.1). The very stable NGTS telescope autoguiding results in stars remaining on the same pixels for the entire observation sequence so that flatfield variations do not contribute any significant photometric noise.

3. NGTS SINGLE TELESCOPE PHOTOMETRIC PRECISION

3.1 Noise model

The precision of the NGTS photometry is well described using a four component noise model comprised of noise from atmospheric scintillation, photon noise of the target star, sky background noise, and the read noise of the CCD camera. Figure 4 sets out these four components for typical observing conditions at the Paranal Observatory: a median sky background (35 ADU/pixel/s) and an airmass of 1.2. The total photometric noise is also shown on Figure 4, which is the sum in quadrature of the four noise components. Scintillation noise is the dominant source of NGTS photometric noise for bright stars (G<12), and is caused by distortion of the star light as it passes through turbulent layers in the Earth's atmosphere. The fractional amplitude of scintillation noise ($\sigma_{\rm Y}$) can be estimated using the modified Young's approximation,[23,24]

$$\sigma_{\rm Y}^2 = 10 \times 10^{-6} C_{\rm Y}^2 D^{-4/3} t^{-1} (\sec z)^3 \exp\left(-2h_{\rm obs}/H\right), \quad (1)$$

where D is the diameter of the telescope aperture (0.2 m for NGTS), t is exposure time used (10 s for NGTS Bright Star observing), $h_{\rm obs}$ is the altitude of the observatory (2440 m for Paranal), H is the scale height of the atmospheric turbulence, taken to be 8000 m. z is the zenith distance, and thus $\sec z$ approximates airmass. $C_{\rm Y}$ ($\rm m^{2/3}s^{1/2}$) is the empirical coefficient that varies depending on the amount of turbulence in the Earth's atmosphere at the time of observation. The median scintillation at Paranal is $C_{\rm Y}$=1.56, with the 1st and 3rd quartiles of 1.37 and 1.76 respectively.[25] For Figure 5 we calculate the scintillation noise assuming the median index of $C_{\rm Y}$=1.56. Unlike the other noise sources, Equation 1 shows that the fractional scintillation noise is independent of the stellar magnitude. This is the reason it dominates the photometric noise for bright stars in NGTS. Equation 1 also shows that scintillation is strongly dependent on airmass, thus NGTS bright star photometry should show much better precision at low airmasses.

The noise model predicts that all bright stars will have a photometric precision of approximately 400 ppm in the assumed observing conditions. The distribution in the photometric precision for bright stars will be set by the variability of the scintillation index at Paranal Observatory during the observation. In fact the NGTS bright star photometry can be used to measure the scintillation index as it applies to the NGTS 10 s imaging (which is known as the "long-exposure" regime).[25]

3.2 Bright Star Sample

To investigate the CCD photometric precision we use NGTS data collected between November 2018 and February 2021. We use observations taken as part of the NGTS "Bright Star" program, which are 10 s exposure time-series observations lasting a minimum of 2 h in duration (though typically 5-6 h). We remove observations taken on nights where the photometry appears to be effected by cloud. Stars brighter than G=7.5 are likely to be saturated at low airmasses in NGTS imaging. Our primary science goals relate to bright star photometry, so we do not include stars fainter than G=12 in our analysis. Therefore our analysis sample contains stars in the magnitude range 7.5<G<12. We also remove stars that show any astrophysical variability in the data - these are predominately pulsating stars, stars with large active regions, or short period binary stars.

All NGTS light curves in our sample are normalized and then de-trended using the sum of all the non-variable bright stars in the frame excluding the target star itself. We calculate the RMS over 30 minute intervals across the normalized light curve. This is a convenient timescale given the typical length of a short period exoplanet transit ($\sim$ 4 h) and also allows us to directly compare to the 30 minute RMS percision calculated for the TESS lightcurves produced by the SPOC pipeline.[26]

In total our sample consists of 21643 light-curves taken from 441 individual telescope pointings on 122 individual nights between November 2018 and February 2021. The sample of lightcurves used in this analysis is identical to the sample used in our study of the scintillation at Paranal.[25]

3.3 Photometric Precision Results

The distribution of our 30-minute RMS photometric precision for the bright star sample is set out in Figure 5. We report two distributions. The first is the *minimum* 30-minute RMS photometric precision, which is calculated for the lowest 30-minute RMS portion of the light-curve. Due to the strong airmass dependence for scintillation noise (Equation 1), this typically occurs when the target is high in the sky near airmass of 1.0. We also present the *mean* 30-minute RMS photometric precision for each light-curve. This measure calculates the noise over the entire light-curve, which will include a range of airmasses, in many cases up to an airmass value of 2.0.

We find a distribution of minimum RMS values that peaks at approximately 400 ppm, which is in good agreement with the prediction from our noise model (see Section 3.1). This implies that for bright stars we do not have any additional sources of noise at the level of ~ 100 ppm. The distribution is approximately Gaussian, although shows a long tail extending to higher RMS values. We attribute this distribution to variability in the scintillation index for Paranal Observatory.[25]

For the mean RMS distribution, we find a very similar distribution to the minimum 30-minute RMS distribution, but the peak is shifted to approximately 550 ppm. This is as expected given the median values will include higher airmass portions of the light-curve.

4. MULTI-TELESCOPE OBSERVATIONS

To detect and characterise very shallow transits we need to achieve better photometric precision than is possible with a single NGTS telescope (typically 400 ppm per 30 minutes; see Section 3 and Figure 5). In order to do this we observe the target star simultaneously with multiple NGTS telescopes - an operational mode named "multi-telescope". This NGTS observing mode was first used in observations of WASP-166[21] and HD106315.[27] In these

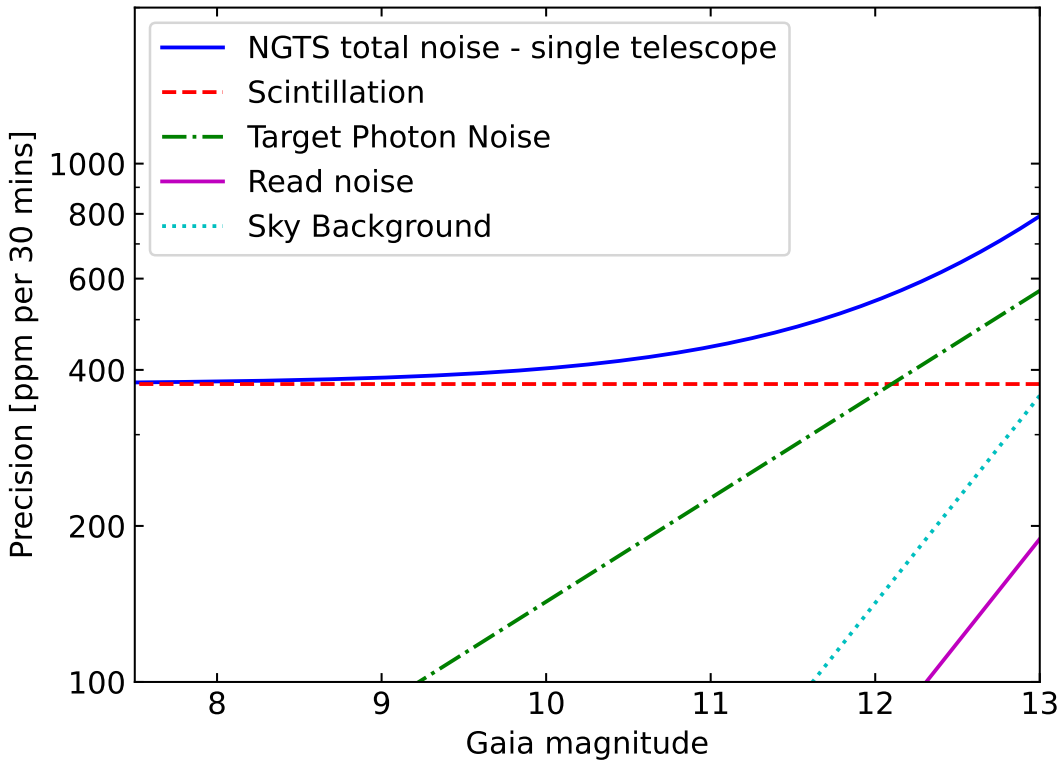

Figure 4. The noise model for NGTS in parts-per-million (ppm) per 30-minutes as a function of stellar magnitude. The solid blue line shows the total noise, with contributions from scintillation (dashed red line), target photon noise (dotted-dashed green line), sky background (dotted pale blue line) and read noise (solid magenta line). We assume the median scintillation conditions at Paranal (C_Y=1.56), a median sky background (35 ADU/pixel/s), and an airmass of 1.2.

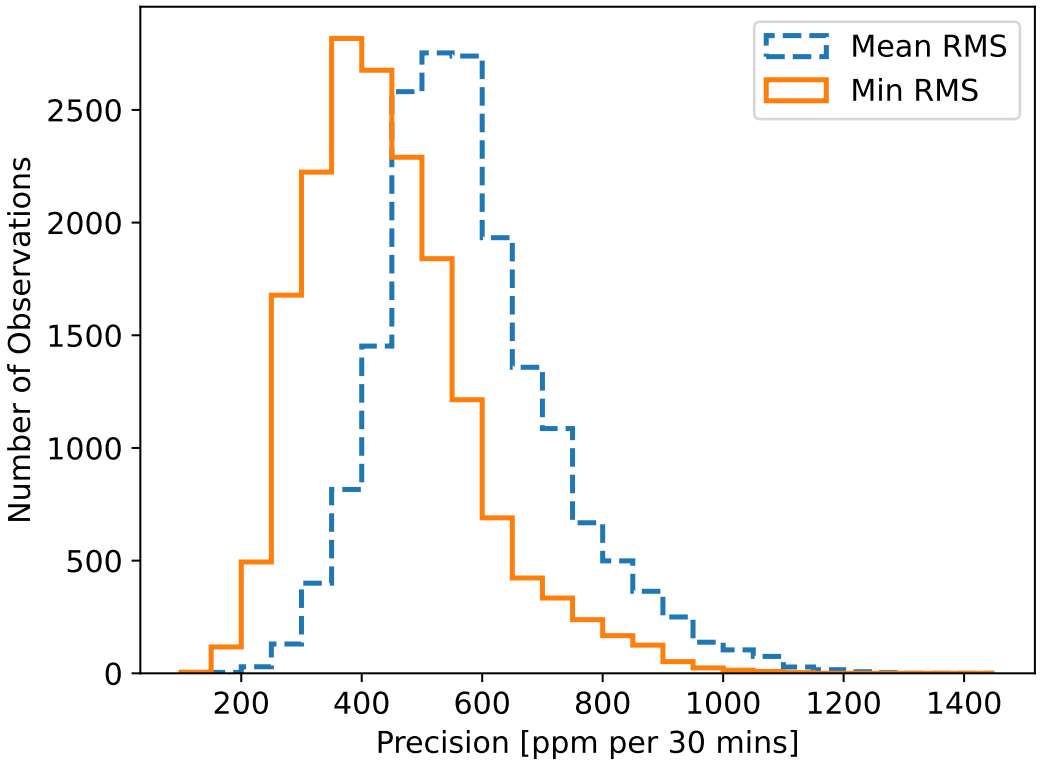

Figure 5. Histogram of 30-minute RMS photometric precision for single NGTS telescope time-series observations of the bright star sample (G<12). The orange (solid line) histogram represents the minimum RMS for a given light curve, which will typically occur at low airmass. The blue (dashed line) histogram represents the mean RMS of the lightcurve, which is taken over the full range of airmasses for each observation.

studies we established that for bright stars (scintillation noise dominated), the photometric noise is completely uncorrelated between individual NGTS telescopes (physically spaced at least 2 m from each other). This allows photometry between N telescopes to be combined to given a $\sqrt{N}$ improvement in the total photometric precision. Figure 6 shows the precision gain for multi-telescope observations assuming standard photometric conditions.

From 2019 onwards, we have been routinely operating NGTS in multi-telescope mode when very high precision is required. An example of a multi-telescope mode in operation is the transiting exoplanet WASP-18b shown in Figure 7, as part of the NGTS search for orbital period decay in ultra-short period transiting exoplanets. The observation was conducted on the night of 2019 October 28 using five NGTS telescopes, and the measured photometric precision is 180 ppm per 30-minutes. Such high precision is essential in order to search for the subtle long term period changes expected from the tidal decay of exoplanet orbits.

The NGTS multi-telescope operation mode has been extremely fruitful for following-up shallow transits from the TESS mission as part of the TESS Follow-Up Observing Program (TFOP)[‡]. These include exciting TESS exoplanet discoveries such as the remnant planetary core TOI-849 b,[28] the ultra-short period planet LTT 9779 b,[29] and the six-planet resonant system TOI-178.[30] In fact, in Figure 8 we show that by using all 12 telescopes, NGTS is able to produce photometric precision equal to or better than TESS for stars as bright as G=9. Real examples of this include systems where NGTS and TESS have simultaneously observed the same transits - such as was the case for WASP-166 b[21] and NGTS-12 b.[31]

[‡]https://tess.mit.edu/followup/

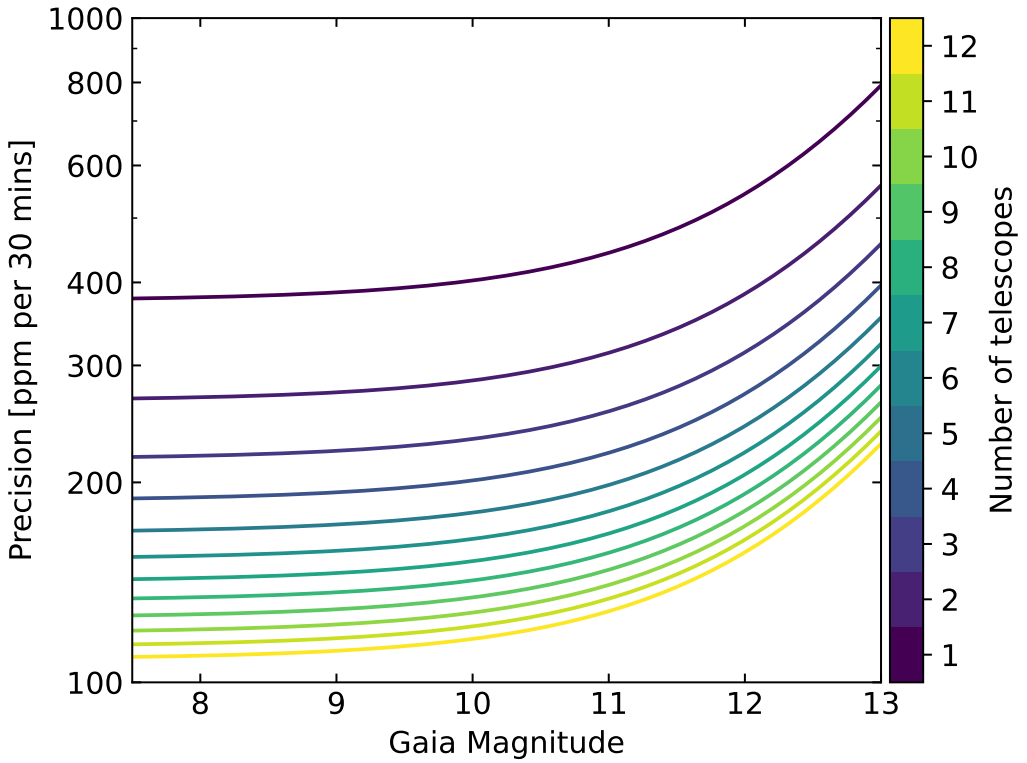

Figure 6. Photometric precision as a function of stellar magnitude for the NGTS multi-telescope observations ranging from 1 to 12 NGTS telescopes (blue to yellow line shading). Assumptions for observing conditions as for Figure 4.

5. SCIENTIFIC CMOS

As discussed in Section 2.1, a camera for astronomical imaging needs to fulfill a set of technical specifications to allow for high precision photometric observations. To date, Charge Coupled Devices (CCDs) are the most popular sensor choice for this type of application. However, due to major technology advancements in the field of Complementary Metal-Oxide-Semiconductor (CMOS) Image Sensors over the past years, scientific CMOS (sCMOS) cameras have gained increasing attention as an alternate high performance imaging solution for several astronomical applications.

In principle, sCMOS cameras provide ideal performance features for high precision photometry as they *simultaneously* offer very low noise, high dynamic range, high sensitivity and resolution, as well as rapid frame rates, large sensor sizes, and shutterless operation. This set of capabilities highlights that performance drawbacks, which have been associated with conventional and previous generations of CMOS sensors, have been overcome and these devices are ready to be used in astronomical applications.[33]

5.1 The Marana 4.2B-11 sCMOS

With the advanced performance features of new sCMOS detectors, we plan to conduct on-sky testing of a new sCMOS camera side-by-side with an existing iKon-L CCD camera at our NGTS facility. The aim is to directly compare and evaluate the detectors' performance for high precision photometry. For these tests we selected the Andor Marana 4.2B-11 BV sCMOS camera, with a sensor size of 22.5×22.5 mm and pixel size of 11 µm. It utilizes the back-illuminated GSense 400BSI detector from Gpixel[§]. The BV sensor option offers high quantum efficiency from 400 to 800nm, which is shown and compared to the iKon-L CCD's sensitivity in Figure 3. The technical specifications of the Marana sCMOS camera are set out in Table 1.

[§]https://www.gpixel.com/

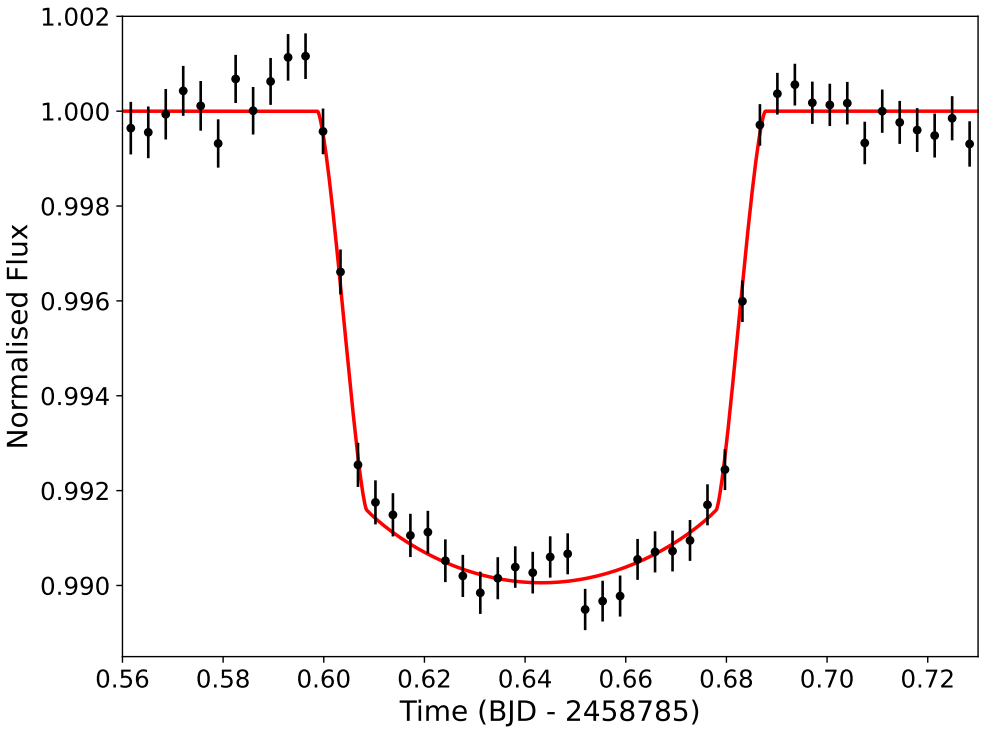

Figure 7. The transit of WASP-18 b from NGTS on the night of 2019 October 28. The observation was made using five NGTS telescopes. Black points are NGTS photometric points binned to 5 minutes. The red line shows the best fit transit model. The photometric precision is 180 ppm per 30-minutes. These observations are part of a long-term program to look for orbital decay in ultra-short period transiting exoplanets.

The read noise is extremely low for sCMOS cameras. The Marana has a read noise of just 1.6 electrons, markedly lower than even the slowest speed, lowest noise CCD modes (see Table 1). While sCMOS cameras show very low read noise properties, deep thermoelectric cooling is required to minimize the contribution of thermal noise and dark current. The Marana sCMOS camera has been designed to offer effective sensor cooling to an absolute sensor temperature of -25°C. In addition, the sensor is protected in a vacuum enclosure based on Andor's UltraVac^{TM} Technology, making it a reliable and low maintenance camera solution.

A comparison of the pixel well depth between the cameras shows that the Marana 4.2B-11 sCMOS has a lower well depth (85,000 electrons) than the iKon-L CCD (150,000 electrons). However, the Marana sCMOS has significantly lower read out noise, especially for high-frame rate measurements (see Table 1). A realistic estimate of dynamic range requires consideration of target frame rate and exposure time, but a rough estimate of maximum pixel well depth divided by minimum read out noise gives nearly equal values for both cameras, approximately 50,000:1. In addition, the Marana sCMOS measurement linearity is specified at $> 99.7\%$ over the full range of the sensor, as defined in the EMVA 1288 standard. Photo Response Non-Uniformity (PRNU) is also minimal, with a value of $< 0.5\%$ at half-saturation.

5.2 Testing the Marana sCMOS at NGTS

We plan to test the photometric performance of the new Marana sCMOS camera for use in the NGTS project. This work will be conducted as a collaboration between NGTS and Andor Technology.

The first phase of the project will involve laboratory testing at the University of Warwick. We will investigate the noise properties of the sCMOS images under the standard NGTS operating conditions and exposure times. This testing will also be important for understanding how to best integrate the sCMOS camera into the existing NGTS software and hardware architecture.

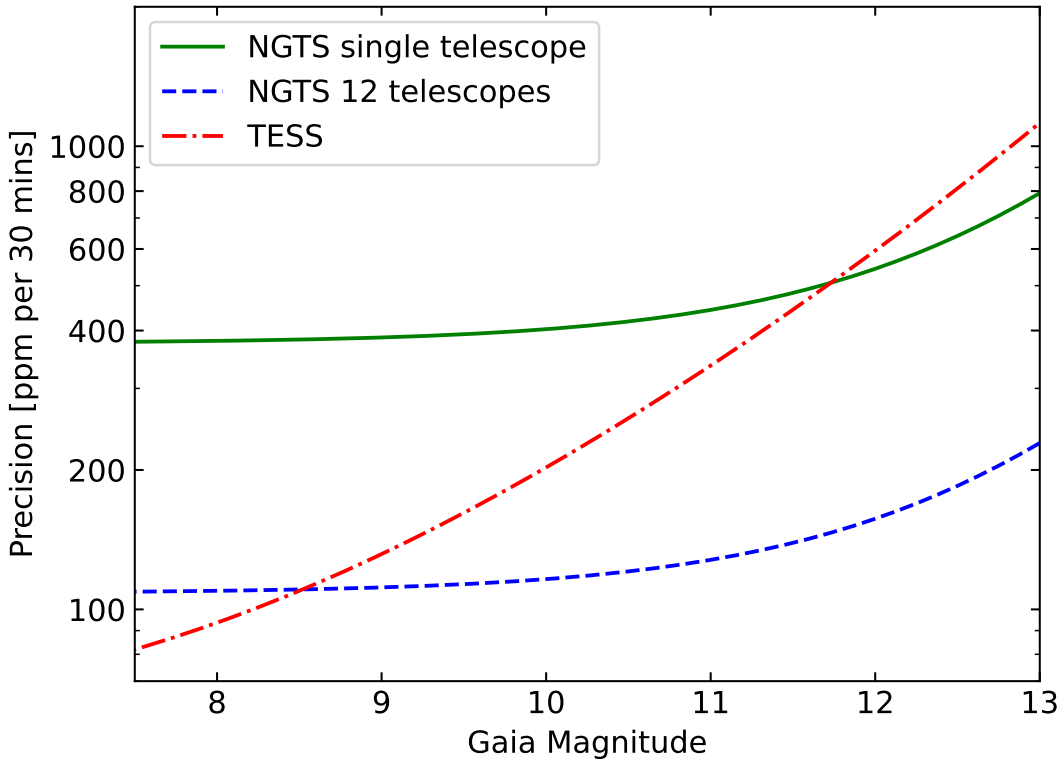

Figure 8. Photometric precision as a function of stellar magnitude for a single NGTS telescope (green line), 12 NGTS operations in multi-telescope mode (blue dashed line) and the TESS spacecraft[32] (red dot-dashed line). Using 12 telescopes NGTS can achieve $\sim$ 100 ppm photometry for bright stars, and is competitive with TESS for stars as bright as G=9. NGTS precision assumes the observing conditions as for Figure 4.

The second phase of the project will be to mount the sCMOS onto an existing NGTS telescope within the NGTS facility at the Paranal Observatory, Chile. The sCMOS will then operate alongside the existing i-Kon-L CCD cameras. We will simultaneously observe stars with both the sCMOS and CCD camera in order to directly compare the photometric precision of the instruments. We will also trial photometry on very bright stars (G<5). This will take advantage of the fast readout capabilities and shutterless operation of the sCMOS camera to use short exposure times of $\sim$1 s (see Table 1). Such photometry has not been feasible with CCD cameras due to the longer readout times and concern for wear on the camera shutter.

In the third and final phase of the project we will use the results of the on-sky testing to investigate if we can improve our photometric precision by modifications to the sCMOS camera hardware, firmware, or data processing. This phase of the project will involve a close collaboration between the University of Warwick and Andor Technology.

6. CONCLUSIONS

NGTS has been operating for 6 years, and is now routinely producing some of the most precise time series photometry of any ground based telescope. For bright stars (G<12) observed at low airmass, we show that our 30 minute RMS precision is 400 ppm, in line with the predicted noise model in the scintillation dominated regime. By using multiple NGTS telescopes this 30 minute RMS precision can be improved to 100 ppm, meaning that NGTS has a similar precision to the TESS mission for stars as bright as G=9. Over the next few years NGTS will continue to discover and characterise transiting exoplanets. We will also test the latest sCMOS camera in order to ascertain if such a camera can match the precision of the current generation of CCD cameras. If sCMOS cameras can reliably produce high precision astronomical photometry they could be coupled with multiple telescope observing modes to create new generations of high precision ground-based photometry facilities.

ACKNOWLEDGMENTS

NGTS is a collaboration between UK Universities Warwick, Leicester, Cambridge, and Queen's University Belfast, together with the Observatoire de Genève, DLR Berlin and Universidad de Chile.

Based on data collected under the NGTS project at the ESO La Silla Paranal Observatory. The NGTS facility is operated by the consortium institutes with support from the UK Science and Technology Facilities Council (STFC) through projects ST/M001962/1, ST/S002642/1 and ST/W003163/1.

NGTS and Andor Technology acknowledge the support of the UK Science and Technology Facilities Council (STFC) under the grants ST/W005077/1 *Precision Photometry with the new generation of fast readout Scientific CMOS Camera* and ST/W005719/1 *Discovering New Worlds with sCMOS Cameras.*

REFERENCES

[1] Struve, O., "Proposal for a project of high-precision stellar radial velocity work," *The Observatory* **72**, 199–200 (Oct. 1952).

[2] Mayor, M. and Queloz, D., "A Jupiter-mass companion to a solar-type star," Nature **378**, 355–359 (Nov. 1995).

[3] Charbonneau, D., Brown, T. M., Latham, D. W., and Mayor, M., "Detection of Planetary Transits Across a Sun-like Star," ApJ **529**, L45–L48 (Jan. 2000).

[4] Henry, G. W., Marcy, G. W., Butler, R. P., and Vogt, S. S., "A Transiting "51 Peg-like" Planet," ApJ **529**, L41–L44 (Jan. 2000).

[5] Pollacco, D. L., Skillen, I., Collier Cameron, A., Christian, D. J., Hellier, C., Irwin, J., Lister, T. A., Street, R. A., West, R. G., Anderson, D. R., Clarkson, W. I., Deeg, H., Enoch, B., Evans, A., Fitzsimmons, A., Haswell, C. A., Hodgkin, S., Horne, K., Kane, S. R., Keenan, F. P., Maxted, P. F. L., Norton, A. J., Osborne, J., Parley, N. R., Ryans, R. S. I., Smalley, B., Wheatley, P. J., and Wilson, D. M., "The WASP Project and the SuperWASP Cameras," PASP **118**, 1407–1418 (Oct. 2006).

[6] Bakos, G., Noyes, R. W., Kovács, G., Stanek, K. Z., Sasselov, D. D., and Domsa, I., "Wide-Field Millimagnitude Photometry with the HAT: A Tool for Extrasolar Planet Detection," PASP **116**, 266–277 (Mar. 2004).

[7] Bakos, G. Á., Csubry, Z., Penev, K., Bayliss, D., Jordán, A., Afonso, C., Hartman, J. D., Henning, T., Kovács, G., Noyes, R. W., Béky, B., Suc, V., Csák, B., Rabus, M., Lázár, J., Papp, I., Sári, P., Conroy, P., Zhou, G., Sackett, P. D., Schmidt, B., Mancini, L., Sasselov, D. D., and Ueltzhoeffer, K., "HATSouth: A Global Network of Fully Automated Identical Wide-Field Telescopes," PASP **125**, 154 (Feb. 2013).

[8] Charbonneau, D., Brown, T. M., Noyes, R. W., and Gilliland, R. L., "Detection of an Extrasolar Planet Atmosphere," ApJ **568**, 377–384 (Mar. 2002).

[9] Knutson, H. A., Charbonneau, D., Allen, L. E., Fortney, J. J., Agol, E., Cowan, N. B., Showman, A. P., Cooper, C. S., and Megeath, S. T., "A map of the day-night contrast of the extrasolar planet HD 189733b," Nature **447**, 183–186 (May 2007).

[10] Stevenson, K. B., Lewis, N. K., Bean, J. L., Beichman, C., Fraine, J., Kilpatrick, B. M., Krick, J. E., Lothringer, J. D., Mandell, A. M., Valenti, J. A., Agol, E., Angerhausen, D., Barstow, J. K., Birkmann, S. M., Burrows, A., Charbonneau, D., Cowan, N. B., Crouzet, N., Cubillos, P. E., Curry, S. M., Dalba, P. A., de Wit, J., Deming, D., Désert, J.-M., Doyon, R., Dragomir, D., Ehrenreich, D., Fortney, J. J., García Muñoz, A., Gibson, N. P., Gizis, J. E., Greene, T. P., Harrington, J., Heng, K., Kataria, T., Kempton, E. M. R., Knutson, H., Kreidberg, L., Lafrenière, D., Lagage, P.-O., Line, M. R., Lopez-Morales, M., Madhusudhan, N., Morley, C. V., Rocchetto, M., Schlawin, E., Shkolnik, E. L., Shporer, A., Sing, D. K., Todorov, K. O., Tucker, G. S., and Wakeford, H. R., "Transiting Exoplanet Studies and Community Targets for JWST's Early Release Science Program," PASP **128**, 094401 (Sept. 2016).

[11] Pont, F., Zucker, S., and Queloz, D., "The effect of red noise on planetary transit detection," MNRAS **373**, 231–242 (Nov. 2006).

[12] Borucki, W. J., Koch, D., Basri, G., Batalha, N., Brown, T., Caldwell, D., Caldwell, J., Christensen-Dalsgaard, J., Cochran, W. D., DeVore, E., Dunham, E. W., Dupree, A. K., Gautier, T. N., Geary, J. C., Gilliland, R., Gould, A., Howell, S. B., Jenkins, J. M., Kondo, Y., Latham, D. W., Marcy, G. W., Meibom, S., Kjeldsen, H., Lissauer, J. J., Monet, D. G., Morrison, D., Sasselov, D., Tarter, J., Boss, A., Brownlee, D., Owen, T., Buzasi, D., Charbonneau, D., Doyle, L., Fortney, J., Ford, E. B., Holman, M. J., Seager, S., Steffen, J. H., Welsh, W. F., Rowe, J., Anderson, H., Buchhave, L., Ciardi, D., Walkowicz, L., Sherry, W., Horch, E., Isaacson, H., Everett, M. E., Fischer, D., Torres, G., Johnson, J. A., Endl, M., MacQueen, P., Bryson, S. T., Dotson, J., Haas, M., Kolodziejczak, J., Van Cleve, J., Chandrasekaran, H., Twicken, J. D., Quintana, E. V., Clarke, B. D., Allen, C., Li, J., Wu, H., Tenenbaum, P., Verner, E., Bruhweiler, F., Barnes, J., and Prsa, A., "Kepler Planet-Detection Mission: Introduction and First Results," *Science* **327**, 977 (Feb. 2010).

[13] Howard, A. W., Marcy, G. W., Bryson, S. T., Jenkins, J. M., Rowe, J. F., Batalha, N. M., Borucki, W. J., Koch, D. G., Dunham, E. W., Gautier, Thomas N., I., Van Cleve, J., Cochran, W. D., Latham, D. W., Lissauer, J. J., Torres, G., Brown, T. M., Gilliland, R. L., Buchhave, L. A., Caldwell, D. A., Christensen-Dalsgaard, J., Ciardi, D., Fressin, F., Haas, M. R., Howell, S. B., Kjeldsen, H., Seager, S., Rogers, L., Sasselov, D. D., Steffen, J. H., Basri, G. S., Charbonneau, D., Christiansen, J., Clarke, B., Dupree, A., Fabrycky, D. C., Fischer, D. A., Ford, E. B., Fortney, J. J., Tarter, J., Girouard, F. R., Holman, M. J., Johnson, J. A., Klaus, T. C., Machalek, P., Moorhead, A. V., Morehead, R. C., Ragozzine, D., Tenenbaum, P., Twicken, J. D., Quinn, S. N., Isaacson, H., Shporer, A., Lucas, P. W., Walkowicz, L. M., Welsh, W. F., Boss, A., Devore, E., Gould, A., Smith, J. C., Morris, R. L., Prsa, A., Morton, T. D., Still, M., Thompson, S. E., Mullally, F., Endl, M., and MacQueen, P. J., "Planet Occurrence within 0.25 AU of Solar-type Stars from Kepler," ApJS **201**, 15 (Aug. 2012).

[14] Wheatley, P. J., West, R. G., Goad, M. R., Jenkins, J. S., Pollacco, D. L., Queloz, D., Rauer, H., Udry, S., Watson, C. A., Chazelas, B., Eigmüller, P., Lambert, G., Genolet, L., McCormac, J., Walker, S., Armstrong, D. J., Bayliss, D., Bento, J., Bouchy, F., Burleigh, M. R., Cabrera, J., Casewell, S. L., Chaushev, A., Chote, P., Csizmadia, S., Erikson, A., Faedi, F., Foxell, E., Gänsicke, B. T., Gillen, E., Grange, A., Günther, M. N., Hodgkin, S. T., Jackman, J., Jordán, A., Louden, T., Metrailler, L., Moyano, M., Nielsen, L. D., Osborn, H. P., Poppenhaeger, K., Raddi, R., Raynard, L., Smith, A. M. S., Soto, M., and Titz-Weider, R., "The Next Generation Transit Survey (NGTS)," MNRAS **475**, 4476–4493 (Apr. 2018).

[15] Bayliss, D., Gillen, E., Eigmüller, P., McCormac, J., Alexander, R. D., Armstrong, D. J., Booth, R. S., Bouchy, F., Burleigh, M. R., Cabrera, J., Casewell, S. L., Chaushev, A., Chazelas, B., Csizmadia, S., Erikson, A., Faedi, F., Foxell, E., Gänsicke, B. T., Goad, M. R., Grange, A., Günther, M. N., Hodgkin, S. T., Jackman, J., Jenkins, J. S., Lambert, G., Louden, T., Metrailler, L., Moyano, M., Pollacco, D., Poppenhaeger, K., Queloz, D., Raddi, R., Rauer, H., Raynard, L., Smith, A. M. S., Soto, M., Thompson, A. P. G., Titz-Weider, R., Udry, S., Walker, S. R., Watson, C. A., West, R. G., and Wheatley, P. J., "NGTS-1b: a hot Jupiter transiting an M-dwarf," MNRAS **475**, 4467–4475 (Apr. 2018).

[16] West, R. G., Gillen, E., Bayliss, D., Burleigh, M. R., Delrez, L., Günther, M. N., Hodgkin, S. T., Jackman, J. A. G., Jenkins, J. S., King, G., McCormac, J., Nielsen, L. D., Raynard, L., Smith, A. M. S., Soto, M., Turner, O., Wheatley, P. J., Almleaky, Y., Armstrong, D. J., Belardi, C., Bouchy, F., Briegal, J. T., Burdanov, A., Cabrera, J., Casewell, S. L., Chaushev, A., Chazelas, B., Chote, P., Cooke, B. F., Csizmadia, S., Ducrot, E., Eigmüller, P., Erikson, A., Foxell, E., Gänsicke, B. T., Gillon, M., Goad, M. R., Jehin, E., Lambert, G., Longstaff, E. S., Louden, T., Moyano, M., Murray, C., Pollacco, D., Queloz, D., Rauer, H., Sohy, S., Thompson, S. J., Udry, S., Walker, S. R., and Watson, C. A., "NGTS-4b: A sub-Neptune transiting in the desert," MNRAS **486**, 5094–5103 (July 2019).

[17] Szabó, G. M. and Kiss, L. L., "A Short-period Censor of Sub-Jupiter Mass Exoplanets with Low Density," ApJ **727**, L44 (Feb. 2011).

[18] Mazeh, T., Holczer, T., and Faigler, S., "Dearth of short-period Neptunian exoplanets: A desert in period-mass and period-radius planes," A&A **589**, A75 (May 2016).

[19] Ricker, G. R., Winn, J. N., Vanderspek, R., Latham, D. W., Bakos, G. Á., Bean, J. L., Berta-Thompson, Z. K., Brown, T. M., Buchhave, L., Butler, N. R., Butler, R. P., Chaplin, W. J., Charbonneau, D., Christensen-Dalsgaard, J., Clampin, M., Deming, D., Doty, J., De Lee, N., Dressing, C., Dunham, E. W., Endl, M., Fressin, F., Ge, J., Henning, T., Holman, M. J., Howard, A. W., Ida, S., Jenkins, J., Jernigan,

G., Johnson, J. A., Kaltenegger, L., Kawai, N., Kjeldsen, H., Laughlin, G., Levine, A. M., Lin, D., Lissauer, J. J., MacQueen, P., Marcy, G., McCullough, P. R., Morton, T. D., Narita, N., Paegert, M., Palle, E., Pepe, F., Pepper, J., Quirrenbach, A., Rinehart, S. A., Sasselov, D., Sato, B., Seager, S., Sozzetti, A., Stassun, K. G., Sullivan, P., Szentgyorgyi, A., Torres, G., Udry, S., and Villasenor, J., "Transiting Exoplanet Survey Satellite (TESS)," in [*Space Telescopes and Instrumentation 2014: Optical, Infrared, and Millimeter Wave*], Oschmann, Jacobus M., J., Clampin, M., Fazio, G. G., and MacEwen, H. A., eds., *Society of Photo-Optical Instrumentation Engineers (SPIE) Conference Series* **9143**, 914320 (Aug. 2014).

[20] McCormac, J., Pollacco, D., Skillen, I., Faedi, F., Todd, I., and Watson, C. A., "DONUTS: A Science Frame Autoguiding Algorithm with Sub-Pixel Precision, Capable of Guiding on Defocused Stars," PASP **125**, 548 (May 2013).

[21] Bryant, E. M., Bayliss, D., McCormac, J., Wheatley, P. J., Acton, J. S., Anderson, D. R., Armstrong, D. J., Bouchy, F., Belardi, C., Burleigh, M. R., Tilbrook, R. H., Casewell, S. L., Cooke, B. F., Gill, S., Goad, M. R., Jenkins, J. S., Lendl, M., Pollacco, D., Queloz, D., Raynard, L., Smith, A. M. S., Vines, J. I., West, R. G., and Udry, S., "Simultaneous TESS and NGTS transit observations of WASP-166 b," MNRAS **494**, 5872–5881 (June 2020).

[22] Bertin, E. and Arnouts, S., "SExtractor: Software for source extraction.," A&AS **117**, 393–404 (June 1996).

[23] Young, A. T., "Photometric error analysis. VI. Confirmation of Reiger's theory of scintillation," AJ **72**, 747 (Aug. 1967).

[24] Osborn, J., Föhring, D., Dhillon, V. S., and Wilson, R. W., "Atmospheric scintillation in astronomical photometry," MNRAS **452**, 1707–1716 (Sept. 2015).

[25] O'Brien, S. M., Bayliss, D., Osborn, J., Bryant, E. M., McCormac, J., Wheatley, P. J., Acton, J. S., Alves, D. R., Anderson, D. R., Burleigh, M. R., Casewell, S. L., Gill, S., Goad, M. R., Henderson, B. A., Jackman, J. A. G., Lendl, M., Tilbrook, R. H., Udry, S., Vines, J. I., and West, R. G., "Scintillation-limited photometry with the 20-cm NGTS telescopes at Paranal Observatory," MNRAS **509**, 6111–6118 (Feb. 2022).

[26] Jenkins, J. M., Twicken, J. D., McCauliff, S., Campbell, J., Sanderfer, D., Lung, D., Mansouri-Samani, M., Girouard, F., Tenenbaum, P., Klaus, T., Smith, J. C., Caldwell, D. A., Chacon, A. D., Henze, C., Heiges, C., Latham, D. W., Morgan, E., Swade, D., Rinehart, S., and Vanderspek, R., "The TESS science processing operations center," in [*Software and Cyberinfrastructure for Astronomy IV*], Chiozzi, G. and Guzman, J. C., eds., *Society of Photo-Optical Instrumentation Engineers (SPIE) Conference Series* **9913**, 99133E (Aug. 2016).

[27] Smith, A. M. S., Eigmüller, P., Gurumoorthy, R., Csizmadia, S., Bayliss, D., Burleigh, M. R., Cabrera, J., Casewell, S. L., Erikson, A., Goad, M. R., Grange, A., Jenkins, J. S., Pollacco, D., Rauer, H., Raynard, L., Udry, S., West, R. G., and Wheatley, P. J., "Shallow transit follow-up from Next-Generation Transit Survey: Simultaneous observations of HD 106315 with 11 identical telescopes," *Astronomische Nachrichten* **341**, 273–282 (Mar. 2020).

[28] Armstrong, D. J., Lopez, T. A., Adibekyan, V., Booth, R. A., Bryant, E. M., Collins, K. A., Deleuil, M., Emsenhuber, A., Huang, C. X., King, G. W., Lillo-Box, J., Lissauer, J. J., Matthews, E., Mousis, O., Nielsen, L. D., Osborn, H., Otegi, J., Santos, N. C., Sousa, S. G., Stassun, K. G., Veras, D., Ziegler, C., Acton, J. S., Almenara, J. M., Anderson, D. R., Barrado, D., Barros, S. C. C., Bayliss, D., Belardi, C., Bouchy, F., Briceño, C., Brogi, M., Brown, D. J. A., Burleigh, M. R., Casewell, S. L., Chaushev, A., Ciardi, D. R., Collins, K. I., Colón, K. D., Cooke, B. F., Crossfield, I. J. M., Díaz, R. F., Delgado Mena, E., Demangeon, O. D. S., Dorn, C., Dumusque, X., Eigmüller, P., Fausnaugh, M., Figueira, P., Gan, T., Gandhi, S., Gill, S., Gonzales, E. J., Goad, M. R., Günther, M. N., Helled, R., Hojjatpanah, S., Howell, S. B., Jackman, J., Jenkins, J. S., Jenkins, J. M., Jensen, E. L. N., Kennedy, G. M., Latham, D. W., Law, N., Lendl, M., Lozovsky, M., Mann, A. W., Moyano, M., McCormac, J., Meru, F., Mordasini, C., Osborn, A., Pollacco, D., Queloz, D., Raynard, L., Ricker, G. R., Rowden, P., Santerne, A., Schlieder, J. E., Seager, S., Sha, L., Tan, T.-G., Tilbrook, R. H., Ting, E., Udry, S., Vanderspek, R., Watson, C. A., West, R. G., Wilson, P. A., Winn, J. N., Wheatley, P., Villasenor, J. N., Vines, J. I., and Zhan, Z., "A remnant planetary core in the hot-Neptune desert," Nature **583**, 39–42 (July 2020).

[29] Jenkins, J. S., Díaz, M. R., Kurtovic, N. T., Espinoza, N., Vines, J. I., Rojas, P. A. P., Brahm, R., Torres, P., Cortés-Zuleta, P., Soto, M. G., Lopez, E. D., King, G. W., Wheatley, P. J., Winn, J. N., Ciardi, D. R., Ricker, G., Vanderspek, R., Latham, D. W., Seager, S., Jenkins, J. M., Beichman, C. A., Bieryla, A., Burke,

C. J., Christiansen, J. L., Henze, C. E., Klaus, T. C., McCauliff, S., Mori, M., Narita, N., Nishiumi, T., Tamura, M., de Leon, J. P., Quinn, S. N., Villaseñor, J. N., Vezie, M., Lissauer, J. J., Collins, K. A., Collins, K. I., Isopi, G., Mallia, F., Ercolino, A., Petrovich, C., Jordán, A., Acton, J. S., Armstrong, D. J., Bayliss, D., Bouchy, F., Belardi, C., Bryant, E. M., Burleigh, M. R., Cabrera, J., Casewell, S. L., Chaushev, A., Cooke, B. F., Eigmüller, P., Erikson, A., Foxell, E., Gänsicke, B. T., Gill, S., Gillen, E., Günther, M. N., Goad, M. R., Hooton, M. J., Jackman, J. A. G., Louden, T., McCormac, J., Moyano, M., Nielsen, L. D., Pollacco, D., Queloz, D., Rauer, H., Raynard, L., Smith, A. M. S., Tilbrook, R. H., Titz-Weider, R., Turner, O., Udry, S., Walker, S. R., Watson, C. A., West, R. G., Palle, E., Ziegler, C., Law, N., and Mann, A. W., "An ultrahot Neptune in the Neptune desert," *Nature Astronomy* **4**, 1148–1157 (Jan. 2020).

[30] Leleu, A., Alibert, Y., Hara, N. C., Hooton, M. J., Wilson, T. G., Robutel, P., Delisle, J. B., Laskar, J., Hoyer, S., Lovis, C., Bryant, E. M., Ducrot, E., Cabrera, J., Delrez, L., Acton, J. S., Adibekyan, V., Allart, R., Allende Prieto, C., Alonso, R., Alves, D., Anderson, D. R., Angerhausen, D., Anglada Escudé, G., Asquier, J., Barrado, D., Barros, S. C. C., Baumjohann, W., Bayliss, D., Beck, M., Beck, T., Bekkelien, A., Benz, W., Billot, N., Bonfanti, A., Bonfils, X., Bouchy, F., Bourrier, V., Boué, G., Brandeker, A., Broeg, C., Buder, M., Burdanov, A., Burleigh, M. R., Bárczy, T., Cameron, A. C., Chamberlain, S., Charnoz, S., Cooke, B. F., Corral Van Damme, C., Correia, A. C. M., Cristiani, S., Damasso, M., Davies, M. B., Deleuil, M., Demangeon, O. D. S., Demory, B. O., Di Marcantonio, P., Di Persio, G., Dumusque, X., Ehrenreich, D., Erikson, A., Figueira, P., Fortier, A., Fossati, L., Fridlund, M., Futyan, D., Gandolfi, D., García Muñoz, A., Garcia, L. J., Gill, S., Gillen, E., Gillon, M., Goad, M. R., González Hernández, J. I., Guedel, M., Günther, M. N., Haldemann, J., Henderson, B., Heng, K., Hogan, A. E., Isaak, K., Jehin, E., Jenkins, J. S., Jordán, A., Kiss, L., Kristiansen, M. H., Lam, K., Lavie, B., Lecavelier des Etangs, A., Lendl, M., Lillo-Box, J., Lo Curto, G., Magrin, D., Martins, C. J. A. P., Maxted, P. F. L., McCormac, J., Mehner, A., Micela, G., Molaro, P., Moyano, M., Murray, C. A., Nascimbeni, V., Nunes, N. J., Olofsson, G., Osborn, H. P., Oshagh, M., Ottensamer, R., Pagano, I., Pallé, E., Pedersen, P. P., Pepe, F. A., Persson, C. M., Peter, G., Piotto, G., Polenta, G., Pollacco, D., Poretti, E., Pozuelos, F. J., Queloz, D., Ragazzoni, R., Rando, N., Ratti, F., Rauer, H., Raynard, L., Rebolo, R., Reimers, C., Ribas, I., Santos, N. C., Scandariato, G., Schneider, J., Sebastian, D., Sestovic, M., Simon, A. E., Smith, A. M. S., Sousa, S. G., Sozzetti, A., Steller, M., Suárez Mascareño, A., Szabó, G. M., Ségransan, D., Thomas, N., Thompson, S., Tilbrook, R. H., Triaud, A., Turner, O., Udry, S., Van Grootel, V., Venus, H., Verrecchia, F., Vines, J. I., Walton, N. A., West, R. G., Wheatley, P. J., Wolter, D., and Zapatero Osorio, M. R., "Six transiting planets and a chain of Laplace resonances in TOI-178," A&A **649**, A26 (May 2021).

[31] Bryant, E. M., Bayliss, D., Nielsen, L. D., Veras, D., Acton, J. S., Anderson, D. R., Armstrong, D. J., Bouchy, F., Briegal, J. T., Burleigh, M. R., Cabrera, J., Casewell, S. L., Chaushev, A., Cooke, B. F., Csizmadia, S., Eigmüller, P., Erikson, A., Gill, S., Gillen, E., Goad, M. R., Grieves, N., Günther, M. N., Henderson, B., Hogan, A., Jenkins, J. S., Lendl, M., McCormac, J., Moyano, M., Queloz, D., Rauer, H., Raynard, L., Smith, A. M. S., Tilbrook, R. H., Udry, S., Vines, J. I., Watson, C. A., West, R. G., and Wheatley, P. J., "NGTS-12b: A sub-Saturn mass transiting exoplanet in a 7.53 day orbit," MNRAS **499**, 3139–3148 (Dec. 2020).

[32] Stassun, K. G., Oelkers, R. J., Pepper, J., Paegert, M., De Lee, N., Torres, G., Latham, D. W., Charpinet, S., Dressing, C. D., Huber, D., Kane, S. R., Lépine, S., Mann, A., Muirhead, P. S., Rojas-Ayala, B., Silvotti, R., Fleming, S. W., Levine, A., and Plavchan, P., "The TESS Input Catalog and Candidate Target List," AJ **156**, 102 (Sept. 2018).

[33] Karpov, S., Bajat, A., Christov, A., Prouza, M., and Beskin, G., "Evaluation of scientific CMOS sensors for sky survey applications," in [*Society of Photo-Optical Instrumentation Engineers (SPIE) Conference Series*], *Society of Photo-Optical Instrumentation Engineers (SPIE) Conference Series* **11454**, 114540G (Dec. 2020).